first computing α (= P_{Na}/P_K, where P is permeability) for internal (i) and external (o) concentrations $[Na]_i$ = 20 mM, $[Na]_o$ = 145 mM, $[K]_o$ = 0 mM, and $[K]_i$ = 140 mM from α = {[145/exp($E_{rev}F/RT$)] − 20}/140 (where F is the Faraday, R is the gas constant, and T is the absolute temperature). Other P_X/P_{Na} values, when $[X]_o$ = 145 mM, $[Na]_i$ = 20 mM, $[K]_i$ = 140 mM, and $[Na]_o$ = $[K]_o$ = $[X]_i$ = 0 mM, were computed from P_X/P_{Na} = {[exp($E_{rev}F/RT$)](20 + 140α)}/145. In order of size (Fig. 3C), X was cesium, methylamine, tris(hydroxymethyl)-aminomethane, tetraethylammonium, and *N*-methyl-D-glucamine. The internal solution also contained 10 mM EGTA and 5 mM Hepes. External solutions also contained 10 mM glucose and normal or low concentrations of divalent cations; pH was maintained at 7.3 with HCl, histidine, or Hepes as required, and the osmolarity of all solutions was 295 to 315.

14. R. J. Evans, *J. Physiol. (London)* **487**, 193P (1995).
15. S. E. Hickman, J. El-Khoury, S. Greenberg, I. Schieren, S. C. Silverstein, *Blood* **84**, 2452 (1994).
16. J. S. Wiley, J. R. Chen, M. B. Snook, G. P. Jamieson, *Br. J. Pharmacol.* **112**, 946 (1994); T. H. Steinberg, A. S. Newman, J. A. Swanson, S. C. Silverstein, *J. Biol. Chem.* **262**, 8884 (1987).
17. The induction and kinetics of this sustained current were the same for inward current at −70 mV and for outward current at 50 mV (n = 3). Indeed, it did not require any current to flow during the first, conditioning agonist applications: when BzATP was applied 4 to 12 times in normal divalent solution while the reversal potential was held (0 mV in NaCl or −90 mV in NMDG), the sustained current was still evoked by the subsequent application of BzATP when the low divalent solution was introduced and the holding potential was set to −70 mV (n = 3; A. Surprenant *et al.*, data not shown).
18. YO-PRO-1 (10 μM; Molecular Probes, Eugene, OR) was added to the superfusion fluid during electrophysiological recordings 3 to 6 min before switching to low divalent solution and washed out upon switching back to normal divalent solution, after which the fluorescent lamp was turned on and cells were examined with a fluorescein isothiocyanate filter. For cell counts, 500 cells per cover slip were counted in each case.
19. R. J. Evans *et al.*, *Mol. Pharmacol.* **48**, 178 (1995).
20. A. Surprenant *et al.*, data not shown.
21. D. W. Choi, *Neuron* **1**, 623 (1988).
22. Abbreviations for the amino acid residues are as follows: A, Ala; C, Cys; D, Asp; E, Glu; F, Phe; G, Gly; H, His; I, Ile; K, Lys; L, Leu; M, Met; N, Asn; P, Pro; Q, Gln; R, Arg; S, Ser; T, Thr; V, Val; W, Trp; and Y, Tyr.
23. We thank A. Brake and D. Julius for $P2X_2$ cDNA and M. J. Solazzo for sequencing. We are indebted to D. Estoppey for cell culture, transfections, and generating stable cell lines.

15 January 1996; accepted 2 April 1996

Requirement for BMP Signaling in Interdigital Apoptosis and Scale Formation

Hongyan Zou and Lee Niswander*

Interdigital cell death leads to regression of soft tissue between embryonic digits in many vertebrates. Although the signals that regulate interdigital apoptosis are not known, BMPs—signaling molecules of the transforming growth factor–β superfamily—are expressed interdigitally. A dominant negative type I BMP receptor (dnBMPR-IB) was used here to block BMP signaling. Expression of dnBMPR in chicken embryonic hind limbs greatly reduced interdigital apoptosis and resulted in webbed feet. In addition, scales were transformed into feathers. The similarity of the webbing to webbed duck feet led to studies that indicate that *BMP*s are not expressed in the duck interdigit. These results indicate BMP signaling actively mediates cell death in the embryonic limb.

Programmed cell death (PCD) or apoptosis is an important aspect of embryonic development. Significant progress has been made in defining the intracellular pathways of PCD [reviewed in (*1*)]; less well understood, however, are the extracellular events that trigger the process. Apoptosis can result from changes in the extracellular environment, such as alterations in cell adhesion or withdrawal of growth factors (*2*). Rather paradoxically, the presence of a growth factor, bone morphogenetic protein 4 (BMP4), has been suggested to mediate apoptosis of neural crest cells in the developing hindbrain of chickens (*3*).

In the developing chick limb, apoptosis occurs in the interdigital region, as demonstrated by vital dye uptake, nuclear fragmentation, DNA laddering, and TUNEL staining (*4, 5*). Recent studies indicate that interdigital apoptosis can be inhibited by peptide inhibitors of the protease family of intracellular CED-3–interleukin-1β converting enzyme (*6*). Possible extracellular signals of interdigital apoptosis include BMP2, BMP4, and BMP7, all of which are expressed in the interdigital tissue before and during regression in the developing mouse and chick limb bud (*7–11*).

We chose to look at the role of BMPs in limb development. One approach to study BMP function is to block BMP signaling at the level of the receptor. Two types of transmembrane serine-threonine kinase receptors are involved in signaling by BMP and other transforming growth factor–β (TGF-β) family members. Upon ligand binding, type II BMP receptor (BMPR-II) associates with type I BMPR (BMPR-I), and this interaction is essential for signal transduction (*12, 13*). By analogy with activation by TGF-β (*14*), it is thought that ligand-induced receptor association leads to phosphorylation of BMPR-I by BMPR-II and initiation of signal transduction by BMPR-I. Two type I BMPRs have been identified, BMPR-IA (ALK3) and BMPR-IB (ALK6). In in vitro binding assays, BMPR-IB (used in the studies reported here) specifically binds BMP2 and BMP4 and binds BMP7 with lower affinity. BMPR-IB does not bind TGF-β or activin (*15*).

A single amino acid substitution within the adenosine triphosphate binding site (K231R, where Lys^{231} is changed to Arg) was made to generate a dominant negative mutant form of mouse BMPR-IB (dnBMPR). The dnBMPR is inactive in an in vitro kinase assay and defective in signal transduction (*16, 17*). Moreover, excess mutant BMPR can compete with endogenous type I receptor for type II receptors and therefore can act as a dominant negative mutation. We chose to generate the single amino acid mutation rather than an intracellular deletion of the kinase domain for several reasons. (i) The K-to-R conservative substitution should not alter the overall conformation of the receptor. (ii) Cellular trafficking of the K231R receptor should not be disrupted, as often happens for intracellular deletion mutations. (iii) Point mutations should not alter the strong interaction between the intracellular domains of the type I and II BMP receptors (*12*).

The mutant receptor construct was cloned into an avian replication-competent retroviral vector (RCAS) (*18*) and used to produce high-titer viral stock (*19*). The virus was microinjected into the region of the right presumptive hind limbs of chick embryos at stages 13 to 15 or into the right hind limb buds of chick embryos at stages 18 to 20; the embryos were then allowed to develop for a total of 10, 15, or 18 days. Similar phenotypes were observed after infection at the different stages.

Infection with dnBMPR produced three major phenotypes: soft tissue syndactyly (webbing), transformation of scales to feathers, and truncation of the digits (Fig. 1). In essentially 100% of the infected limbs (n > 70), the interdigital tissue did not regress properly and thus the digits were joined by extensive webbing. Embryos examined as late as days 15 and 18 showed persistence of webbing (*20*). We never observed fusion of the digits or ectopic cartilage nodules in the infected foot plates. Extensive webbing was observed in limbs in which the digits were not truncated (Fig. 1, A and B) (*20*), thus indicating that the absence of cell death is not due to an inhibition of growth or cartilage differentiation (*21*). Control infections with RCAS encoding alkaline

Molecular Biology Program, Memorial Sloan-Kettering Cancer Center, 1275 York Avenue, New York, NY 10021, USA, and Graduate School of Medical Sciences, Cornell University, 445 East 69th Street, New York, NY 10021, USA.

*To whom correspondence should be addressed. E-mail: L-niswander@ski.mskcc.org

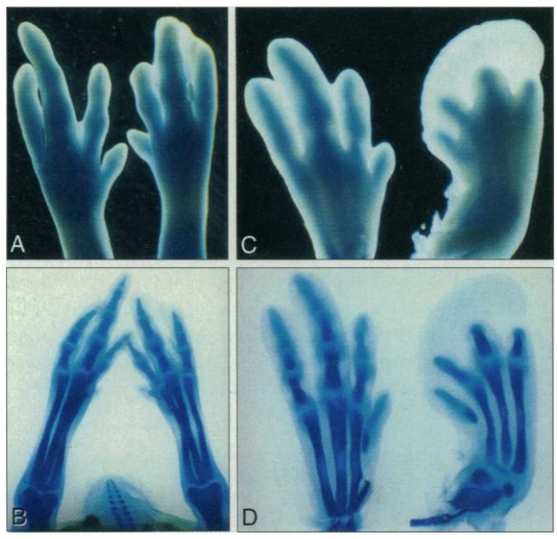

Fig. 1. Infection with dnBMPR-IB of the embryonic chick leg causes webbing and digit truncation. Right hind limb buds were infected at the designated stage (*29*), and the embryos were fixed on embryonic day 10, stained with Alcian Blue to reveal the cartilage, and photographed before (**A** and **C**) and after (**B** and **D**) the tissue was cleared. The predominantly infected leg is on the right, and the contralateral leg from the same embryo is on the left. Infection was at stage 14 in (A) and (B) and at stage 19 in (C) and (D). In (C), all digits were severely truncated such that only the proximal phalanges were formed, whereas in (A) only the most distal phalange of digit 3 was missing. With the use of a picospritzer and micromanipulator, ~3 μl total of viral stock was delivered to multiple sites within the presumptive right hind limb field (caudal to the umbilical vein) of white leghorn embryos from stages 13 to 15 (SPAFAS flock 76 and 77) or the right hind limb bud from stages 18 to 20. Infection at stages 13 to 15 resulted in extensive infection of the right leg by stages 21 to 24, 36 to 48 hours after injection, as analyzed by in situ hybridization with the mouse BMPR-IB complementary DNA, which does not detect chick BMPR-related sequences (*20*). The left leg was also often infected because of the injection protocol and subsequent viral spread, but the extent of infection was variable. Infection at stages 19 and 20 results in an infection that is predominantly limited to the targeted limb. Control infections with RCAS, which encodes alkaline phosphatase, confirmed the extent of infection.

phosphatase, wild-type BMPR-IB, or dnBMPR-IA (single amino acid substitution) did not affect regression of the interdigital tissue (*20*) ($n > 30$ for each control). Interdigital tissue is normally removed by apoptotic cell death. The persistence of interdigital cells in the infected limb correlates with a reduction in apoptosis as analyzed by TUNEL staining, which labels apoptotic cells. As shown in Fig. 2, apoptosis is greatly reduced in dnBMPR-infected limbs (average, <14% and 33% TUNEL-positive cells in dnBMPR and contralateral limb, respectively). *BMP* is normally expressed in the interdigital region. This, coupled with the ability of dnBMPR to cause a reduction in apoptosis and produce soft tissue syndactyly, indicates that BMP signaling is required for developmentally programmed cell death in the interdigital region.

The dnBMPR-induced webbed chick foot is reminiscent of a webbed duck foot, which undergoes relatively little interdigital cell death compared to that in the chick (*4*). Therefore, we performed RNA in situ hybridization to determine whether *BMP* is expressed in the interdigital region of a duck limb bud. In both chick and duck, *BMP2*, *BMP4*, and *BMP7* are expressed in similar tissues—for example, the apical ectodermal ridge, the anterior and posterior mesenchyme (overlapping regions of PCD), the tail bud, and facial processes [Fig. 3, A, B, E, and F (*20*)]. However, *BMP* was not detected in the interdigital region of the duck limb bud ($n > 5$ for each probe), whereas it was readily detected in the chick limb [Fig. 3, C, D, and G (*20*)]. The in situ hybridizations of duck were overexposed to reveal a weak interdigital signal, but none was detected (up to four times as long as required for detection of RNA in the duck apical ridge and in the chick interdigital region). Because PCD between digits 2 and 3, and 3 and 4, in the duck foot occurs in mesenchyme directly underlying the apical ridge, the apoptotic signal may be sent by the ridge, not from within the interdigital mesenchyme.

Expression of *BMP* in the ridge and anterior mesenchyme, as well as the apparent lack of interdigital mesenchyme expression, corresponds with the restricted regions of apoptosis observed in the duck leg. Thus, BMP signaling may mediate PCD in both the chick and duck leg. These data indicate that in at least one case (duck), the relative lack of interdigital apoptosis correlates with the lack of interdigital *BMP* expression,

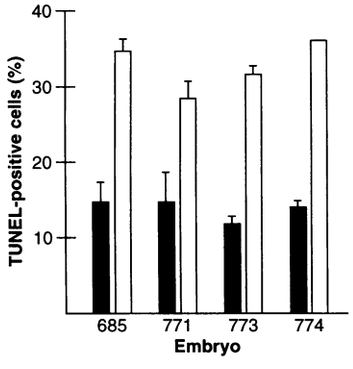

Fig. 2. Apoptosis is reduced in dnBMPR-IB–infected limbs (black bars) compared to that in contralateral limbs (white bars). Total number of cells counted in sections (dnBMPR-infected limb: contralateral limb) are as follows: embryo 685, 3085:1841; embryo 771, 1269:2068; embryo 773, 688:1681; and embryo 774, 1672:747. Note that many sections through the interdigital region of dnBMPR-infected limbs had little or no TUNEL-positive cells. Data were collected from sections displaying the largest number of TUNEL-positive cells for both infected and contralateral limbs.

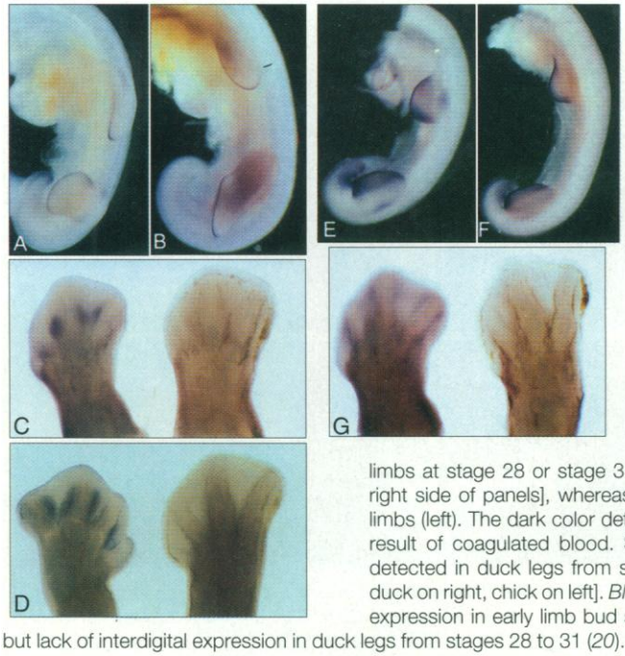

Fig. 3. *BMP* was not expressed in duck interdigital tissue. Shown are whole-mount RNA in situ hybridizations with digoxygenin-labeled probe for chick *BMP4* (**A** through **D**) and *BMP7* (**E** through **G**). *BMP* RNA was detected (purple stain) in the apical ectodermal ridge of chick [(A) and (E)] and duck [(B) and (F)] embryos at stages 25 and 22, respectively, as well as in tail bud, anterior and posterior limb mesenchyme, and facial processes (not shown). In contrast, *BMP4* was not detected in the interdigital region of duck hind limbs at stage 28 or stage 31–32 [(C) and (D), respectively, right side of panels], whereas it was detected in chick hind limbs (left). The dark color detected along the phalanges is a result of coagulated blood. Similarly, *BMP7* RNA was not detected in duck legs from stages 27 to 31 [(G), stage 30: duck on right, chick on left]. *BMP2* also displayed comparable expression in early limb bud stage chick and duck embryos but lack of interdigital expression in duck legs from stages 28 to 31 (*20*). RNA in situ hybridizations were performed as described (*30*) except that the hybridization temperature was 60°C for duck embryos and 70°C for chick embryos. The chick *BMP* probes were prepared as described (*9*, *31*).

whereas in species that undergo interdigital apoptosis (chick and mouse), *BMP* is expressed interdigitally.

In 100% of cases examined at embryonic days 15 and 18, the large scales (scuta) that normally form over the dorsal surface of the foot were at least partially replaced by feathers. Transformations ranged from thickening of the distal edge of the scale to short, fat feathers to long, thin feather filaments (Fig. 4, B through D). As shown additionally by high-power magnification (Fig. 4D), sections through the thin and fat feather filaments (Fig. 4, F and G) revealed the presence of barb ridges characteristic of feathers. However, the number of barb ridges within both the thin and fat filaments was significantly greater than the normal number (up to 40 barb ridges; compare Fig. 4, F and G, to Fig. 4E). The interior pulp region was greatly expanded in the fat filaments. To a much lesser extent we observed the conversion of scutellae to short feather filaments but did not observe conversion of reticula (*20*). Scutellae and reticula are the smaller scales on the posterior and plantar surfaces, respectively. The conversion of scales to feathers is similar to that observed after retinoic acid treatment (*22*). Dhouailly has suggested (*22*) that scale formation requires additional information to override the latent ability of foot integument to produce feathers. Our study also indicates a binary decision between the choice of scale or feather, such that high levels of BMP signaling may be required for scale formation or that scale morphogenesis may be specifically mediated through BMPR-IB.

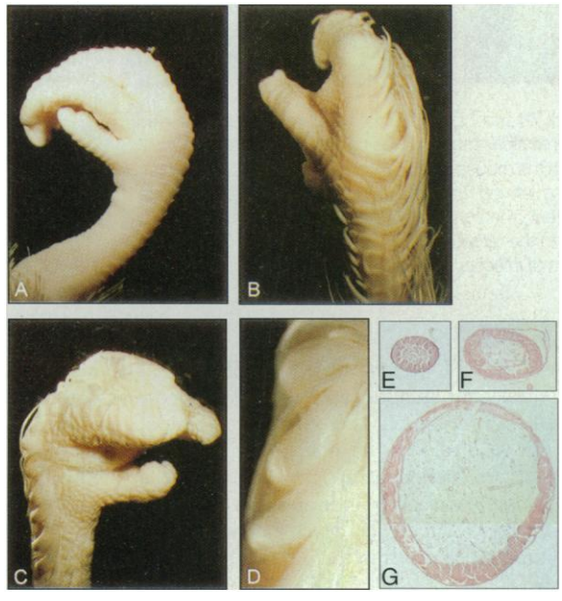

Fig. 4. Transformation of dorsal scales to feather filaments. Embryonic feet from (**A**) control, noninfected embryo and (**B** and **C**) two different embryos infected with dnBMPR-IB at stages 15 and 14, respectively. The embryos in (A) and (B) were fixed on embryonic day 14.5, and that in (C), on embryonic day 18. Note the range of transformation from thickening of the distal edge of the scale to short, fat feathers to long, thin feather filaments. (**D**) Higher magnification of fat feather filaments shown in (C). Cross sections through both the thin and fat feathers (**F** and **G**, respectively) revealed barbed ridges characteristic of feather filaments, although the number of ridges is greater than in normal filaments (compare to that shown in **E**); magnification in (E) through (G) was ×200. The interior pulp region was greatly expanded in the fat filaments. In (B) is partial webbing, whereas in (C) is shown extensive soft-tissue syndactyly. Similar phenotypes were observed on embryonic days 15 and 18 ($n > 7$ for each time point).

Fig. 5. Gene expression after dnBMPR infection. The right hind limb was infected at the designated stage and embryos fixed at stage 32 (*MSX1, MSX2, BMP4*) or stage 26 (*HOXD13*) and processed for whole-mount RNA in situ hybridization with *MSX1*, stage 14; *MSX2*, stage 13; *BMP4*, stage 15; and *HOXD13*, stage 14. Probes were prepared as described (*9, 26, 28*). In each panel, the predominantly infected limb is on the right and the contralateral control on the left.

The third major phenotype observed after dnBMPR-IB infection was an alteration in the distal outgrowth of the digits. The digits were often distally incomplete, ranging from loss of all but the most proximal phalanges to less severe truncations in which only the most distal phalanges were missing [Fig. 1, C and D (*20*)]. Digit truncations, but never interdigital webbing, were also observed after infection with wild-type BMPR-IB. Therefore, digit truncation does not appear to correlate with the presence of dominant negative BMPR. Instead, overexpression of BMPR-IB (dominant negative or wild-type) may disrupt the balance of available receptors and perturb signaling through other receptor-ligand combinations. For example, excess BMPR-IB may titrate the type II receptor, which mediates signaling through a different ligand–type I receptor complex. Thus, the formation of distal phalanges may require specific ligand-receptor interactions. Studies of other BMP-related genes (*BMP5* and *GDF5*) have indicated that specific ligands control the development of different cartilage elements (*23*).

Several other phenotypes were observed. Examination of webbed feet from embryonic days 15 and 18 revealed that the distal-most structure, the claw, was often not formed, but that the ventral toe pads were similar in infected and noninfected feet. The tail was severely truncated in ~10% of the embryos infected at stages 13 to 15, most likely because of the spread of the dnBMPR retrovirus into the developing tail bud (*20*). Skeletal examination revealed that a number of sacral vertebrae were missing, although the pelvis appeared normal. This may indicate that BMP signaling is necessary for normal development of the tail bud mesenchyme or subsequent differentiation of the vertebrae. It is interesting to note that mouse embryos homozygous for a targeted mutation of *BMP4* are deficient in mesoderm production and display truncation of the posterior body axis (*24*). The manner in which the responding cell perceives the BMP signal most likely depends on multiple factors, such as cell history and other stimuli that it receives. In the mouse limb bud, BMPR-IB is expressed in differentiating chondrocytes (*25*). However, histological analysis of dnBMPR-infected limbs from embryonic days 10, 15, and 18 indicates that cartilage and bone differentiation and tendon formation occur normally.

We analyzed the expression of a number of genes that are normally detected in the chick interdigital tissue: *MSX1*, *MSX2*,

BMP2, *BMP4*, and *BMP7* (*9*, *10*, *26*). In dnBMPR-infected limbs, all RNAs are detected at relatively normal levels in the webbed interdigital tissue except *MSX2*, which is at lower levels compared to that in the wild-type limbs (Fig. 5) (*20*). In all cases, the expression pattern was altered such that these RNAs were detected in soft tissue distal to the truncated digits as well as in the interdigital tissue. In addition, *BMP4* RNA was noticeably absent in mesenchyme surrounding the phalanges of infected limbs at later developmental stages. There is evidence to indicate that *BMP4* regulates its own expression (*8*, *27*). Perhaps the lack of phalangeal expression is related to the reduction in BMP signaling caused by the dnBMPR. *HOXD13*, which may be involved in growth and patterning of the phalanges, was expressed similarly in infected and noninfected limbs at stage 26 and stage 32 of limb development, as was *HOXD11* (Fig. 5) (*20*, *28*).

Here, we used a dominant negative BMP receptor to block BMP signaling in the developing limb. Infection with dnBMPR-IB consistently resulted in a reduction in apoptosis that led to soft tissue syndactyly. Moreover, scales were converted into feathers, and distal development of the digits was affected, leading to loss of the distal phalanges. It was not possible to determine whether the dominant negative BMPR inhibited apoptosis by blocking the action of a single BMP ligand or whether different BMP ligands acted in combination. However, BMP4 is an attractive candidate for mediating cell death in the limb. Expression of *BMP4* correlates closely with regions of PCD in the limb: the anterior and posterior necrotic zone and the interdigital region. Moreover, BMP4 has recently been implicated in apoptosis of neural crest cells in the hindbrain in chickens (*3*). Taken together, this evidence suggests that BMP4 may play an important role in mediating apoptosis in different tissues at different times during embryogenesis. Moreover, our results indicate that a functional type I BMP receptor is required for BMP-mediated apoptosis. The interdigital region provides a model in vivo system to potentially link an extracellular apoptotic signal and transmembrane receptor kinase to the downstream intracellular cell death machinery.

Note added in proof: Subsequent experiments in our laboratory using chicken dnBMPR-IB (K231R) result in similar phenotypes as infection with the mouse dnBMPR-IB.

REFERENCES AND NOTES

1. S. J. Korsmeyer, *Trends Genet.* **11**, 101 (1995); M. Whyte and G. Evan, *Nature* **376**, 17 (1995).
2. M. C. Raff, *Nature* **356**, 397 (1992); E. Ruoslahti and J. C. Reed, *Cell* **77**, 477 (1994).
3. A. Graham, P. Francis-West, P. Brickell, A. Lumsden, *Nature* **372**, 684 (1994).
4. J. W. Saunders Jr. and J. F. Fallon, in *Major Problems in Developmental Biology*, M. Locke, Ed. (Academic Press, New York, 1967), pp. 289–314.
5. V. Garcia-Martinez *et al.*, *J. Cell Sci.* **106**, 201 (1993); Z. F. Zakeri, D. Quaglino, T. Latham, R. A. Lockshin, *FASEB J.* **7**, 470 (1993).
6. C. E. Milligan *et al.*, *Neuron* **15**, 385 (1995).
7. K. M. Lyons, R. W. Pelton, B. L. M. Hogan, *Development* **109**, 833 (1990).
8. C. M. Jones, K. M. Lyons, B. L. M. Hogan, *ibid.* **111**, 531 (1991).
9. P. H. Francis, M. K. Richardson, P. M. Brickell, C. Tickle, *ibid.* **120**, 209 (1994).
10. P. H. Francis-West *et al.*, *Dev. Dyn.* **203**, 187 (1995).
11. K. M. Lyons, B. L. M. Hogan, E. J. Robertson, *Mech. Dev.* **50**, 71 (1995).
12. F. Liu, F. Ventura, J. Doody, J. Massagué, *Mol. Cell. Biol.* **15**, 3479 (1995).
13. B. L. Rosenzweig *et al.*, *Proc. Natl. Acad. Sci. U.S.A.* **92**, 7632 (1995).
14. J. L. Wrana, L. Attisano, R. Wieser, F. Ventura, J. Massagué, *Nature* **370**, 341 (1994).
15. B. B. Koenig *et al.*, *Mol. Cell. Biol.* **14**, 5961 (1994); P. ten Dijke *et al.*, *J. Biol. Chem.* **269**, 16985 (1994).
16. H. Zou, L. Niswander, F. Ventura, J. Massagué, unpublished observations.
17. J. Carcamo *et al.*, *Mol. Cell. Biol.* **14**, 3810 (1994).
18. S. H. Hughes, J. J. Greenhouse, C. J. Petropoulos, P. Sutrave, *J. Virol.* **61**, 3004 (1987).
19. The gene encoding mouse BMPR-IB was subjected to site-directed oligo mutagenesis (Clonetech) to change Lys^{231} to Arg. This was cloned into a Cla12Nco shuttle vector and then into the replication-competent avian retroviral vector RCAS(A) (*18*). Primary chick embryo fibroblasts were transfected with the use of lipofectin (Gibco-BRL), culture supernatant was collected on days 6 to 10, and the virus was concentrated by centrifugation, resuspended in a small volume, aliquoted, and stored at −70°C. The concentration of virus was estimated on the basis of reverse transcriptase assays (>1×10^6 units of reverse transcriptase per microliter of concentrated stock), which correlates to ~1×10^{11} plaque-forming units per milliliter of concentrated stock as titered on our indicator virus. Four virus preparations were used for these studies with similar results.
20. H. Zou and L. Niswander, unpublished observations.
21. M.-P. Pautou, *J. Embryol. Exp. Morphol.* **34**, 511 (1975).
22. D. Dhouailly, M. H. Hardy, P. Sengel, *ibid.* **58**, 63 (1980).
23. D. M. Kingsley *et al.*, *Cell* **71**, 399 (1992); E. E. Storm *et al.*, *Nature* **368**, 639 (1994).
24. G. Winnier, M. Blessing, P. A. Labosky, B. L. M. Hogan, *Genes Dev.* **9**, 2105 (1995).
25. Y. Ishidou *et al.*, *J. Bone Miner. Res.* **10**, 1651 (1995).
26. B. Robert, G. Lyons, B. K. Simandl, A. Kuroiwa, M. Buckingham, *Genes Dev.* **5**, 2363 (1991); M. A. Ros, D. Macias, J. F. Fallon, J. M. Hurle, *Anat. Embryol.* **190**, 375 (1994).
27. S. Vainio, I. Karavanova, A. Jowett, I. Thesleff, *Cell* **75**, 45 (1993).
28. J.-C. Izpisúa-Belmonte, C. Tickle, P. Dollé, L. Wolpert, D. Duboule, *Nature* **350**, 585 (1991).
29. V. Hamburger and H. Hamilton, *J. Morphol.* **88**, 49 (1951).
30. D. G. Wilkinson, in *In Situ Hybridization*, D. G. Wilkinson, Ed. (Oxford Univ. Press, Oxford, 1993), pp. 75–83.
31. B. Houston, B. H. Thorp, D. W. Burt, *J. Mol. Endocrinol.* **13**, 289 (1994).

32. We are grateful to K. Miyazono for the gene encoding mouse BMPR-IB, J. Massagué and F. Ventura for receptor construct design and for performing the in vitro kinase assay, and K. Manova of the Memorial Sloan-Kettering Cancer Center Molecular Cytology Facility. Probes were kindly provided by B. Robert (*MSX1* and *MSX2*), P. Brickell (*BMP2* and *BMP4*), B. Houston (*BMP7*), and J.-C. Izpisúa-Belmonte (*HOXD13*). We thank our lab members, B. Hogan and J. Massagué, for critical reading of the manuscript and S. Noramly for advice on the scale-to-feather transformation. This work was supported by Memorial Sloan-Kettering Cancer Center Support Grant and American Cancer Society Junior Faculty Research Award.

2 January 1996; accepted 29 March 1996

Role of Gene Interactions in Hybrid Speciation: Evidence from Ancient and Experimental Hybrids

Loren H. Rieseberg,* Barry Sinervo, C. Randal Linder, Mark C. Ungerer, Dulce M. Arias

The origin of a new diploid species by means of hybridization requires the successful merger of differentiated parental species' genomes. To study this process, the genomic composition of three experimentally synthesized hybrid lineages was compared with that of an ancient hybrid species. The genomic composition of the synthesized and ancient hybrids was concordant ($r_s = 0.68$, $P < 0.0001$), indicating that selection to a large extent governs hybrid species formation. Further, nonrandom rates of introgression and significant associations among unlinked markers in each of the three synthesized hybrid lineages imply that interactions between coadapted parental species' genes constrain the genomic composition of hybrid species.

Reduced hybrid fertility or viability appears to result from unfavorable interactions between parental species' genomes (*1*). As a result, species' genomes are considered to be coadapted and thereby resistant to the introgression of alien genes (*1*). However, the successful origin of new diploid species by means of hybridization raises the possibility that interactions between parental species' genes are not universally unfavorable (*2*). Little is known about the strength and fitness consequences of gene interactions in hybrids or their role in hybrid speciation (*3*). Here we compare

L. H. Rieseberg, B. Sinervo, C. R. Linder, M. C. Ungerer, Department of Biology, Indiana University, Bloomington, IN 47405, USA.
D. M. Arias, Centro de Investigación Ambiental E Investigación Sierra de Huautla, Universidad Autónoma del Estado de Morelos, Cuernavaca, Morelos, Mexico 62210.

*To whom correspondence should be addressed.